# Electrochemical and Optical Properties of Microwave Assisted $MoS_2$ Nanospheres for Solar Cell Application

Shreya Sharma, Peeyush Phogat, Ranjana Jha, Sukhvir Singh*

Research Lab for Energy Systems, Department of Physics, Netaji Subhas University of Technology, New Delhi, India

* Corresponding author. email: sukhvirster@gmail.com

Manuscript submitted March 10, 2023; revised April 18, 2023; accepted May 10, 2023; published July 3, 2023.

doi: 10.12720/sgce.12.3.66-72

**Abstract:** In the present work, $MoS_2$ nanospheres are synthesized via facile microwave assisted hydrothermal route and characterized by structural, optical and morphological analysis. The values of the band gap and refractive index calculated by UV-vis analysis is comparable to the corresponding values of silicon. The morphology is investigated by FESEM images which show the formation of nanospheres along with the presence of Mo and S elements as revealed by EDX. The electrochemical analysis is performed by plotting cyclic voltammograms for different scan rates which show the reversibility of the redox reaction. The linear relationship of the current with scan rate obeying Rendle Sevick equation reveals the diffusion-controlled reaction. Thus, this work confirms the possible use of the molybdenum disulfide as an alternative of the silicon in the solar cells.

**Key words**: Solar cell, electrochemical study, cyclic voltammetry, diffusion behaviour, hydrothermal, microwave synthesis.

## 1. Introduction

Molybdenum disulfide or commonly known as molybdite ($MoS_2$) is a semiconducting material, largely explored for a variety of applications viz. optoelectronics, catalysis, lubrication, gas sensing, Li-ion batteries, etc [1]–[3]. It has a band gap of 1.2 eV in bulk form and 1.6 eV in monolayer form. It has a layered structure like other transition metal dichalcogenides [4], each layer consisting a hexagonal packed layer of Mo atoms sandwiched between two layers of S atoms which resembles the structure of layered graphene. The weak Van der waal forces act between two sulfur terminated layers due to which the layers can slide over each other making it a good lubricant. It exists in three structural forms, 1T, 2H and 3R-$MoS_2$. 1T and 3R states are metastable forms while 2H is thermodynamically and chemically stable state which exists in P6/mmc space group [5].

The electrochemical properties of $MoS_2$ have largely been investigated to explore its usage for optoelectronics and batteries. Sun *et al*. has shown that the large surface area of $MoS_2$ nanostructures exhibits large electrocatalytic activity and good reversibility [6]. It also exhibits diffusion-controlled behaviour. All these properties make $MoS_2$, a promising candidate for solar cells.

It can be synthesized by numerous techniques like hydrothermal, chemical vapor deposition, microwave synthesis, hot injection method, etc [7]–[9]. Microwave assisted hydrothermal route is an emerging technique in which microwave treatment is given prior to the hydrothermal process. It increases the reaction rate of the synthesis and reduces the band gap. The present work reports the synthesis of $MoS_2$ nanospheres via microwave assisted hydrothermal method and its electrochemical study for the

prospective use in the solar cells.

## 2. Experimental Section

### 2.1. Chemicals and reagents

Ammonium molybdate tetrahydrate ($(NH_4)_6Mo_7O_{24}.4H_2O$), thiourea ($CH_4N_2S$) and Polyvinylpyrrolidone (PVP) are purchased from Sigma-Aldrich. Distilled water (>5 MΩ) obtained from Millipore is used for the synthesis. Absolute ethanol (99%) is also used when required. The chemicals and reagents used for synthesis are of high purity and analytical grade and used without further purification.

### 2.2. Synthesis of $MoS_2$ nanospheres

$(NH_4)_6Mo_7O_{24}.4H_2O$ (0.03 M) is added to DI water and stirred for few minutes. $CH_4N_2S$ (0.43 M) and PVP are dissolved in the former solution along with continuous stirring. The solution is then irradiated with the microwave radiations of frequency 2450 MHz and power 1800 watt. It is then kept in the Teflon lined autoclave at 220°C for 18 hours. The Teflon is kept undisturbed to cool down naturally and centrifuged. Finally, the sample is dried at 60°C and collected for characterizations and further use.

### 2.3. Deposition of thin film

The film of the as-synthesized sample is deposited on fluorine doped tin oxide (FTO) glass substrate by spin coating technique. Few drops of the sample solution are dispensed on the substrate spinning at high rpm and dried for few minutes. The cycle is repeated several times to get a thin and uniform film.

## 3. Results and Discussion

### 3.1. Structural analysis

The as-synthesized sample is structurally analyzed by utilizing X-ray Diffraction (XRD) technique (PANalytical X'pert PRO facility). The obtained XRD pattern (Fig. 2) is matched with ICDD database code 00-002-1133 and the structural parameters are studied. The as-synthesized sample is indexed to hexagonal (2H) $MoS_2$ phase and P63/mmc space group. The indexed space group depicts the layered hexagonal structure as two m's denote the mirror planes perpendicular and parallel to c-axis respectively while c indicates the glide planes. The diffused pattern and broad peaks reveal the low crystallinity of $MoS_2$ which is also confirmed by the shiny and glassy look of the powder obtained. The broadening of peaks also suggests the nano size $MoS_2$ particles. (002) and (100) peaks correspond to the extension along c- and a-directions respectively. The shift in (002) peak towards low angle from 13.4° to 11.9° indicates the increased interlayer distance.

The lattice parameters of the as-synthesized nanoparticles are calculated using the d-spacing values and indexed miller indices which are compared with the standard data as reported in Table 1. Here, the calculated value of 'c' is larger than the standard value confirming the above inference of larger interlayer distance. The crystallite size is calculated using Debye Scherrer equation to confirm the nano-sized particles. It ranges from 88 to 100 nm for individual peaks and the average crystallite size as calculated is found to be 94.76 nm. XRD data is also exploited to estimate other parameters which include dislocation density in the material, stacking fault and microstrain due to dislocations using the following equations.

$$\delta = \frac{1}{D^2} \tag{1}$$

$$\varepsilon = \frac{\beta \cos\theta}{4} \tag{2}$$

$$\sigma = \frac{2\pi^2}{45(3\tan\theta)^{1/2}}\beta \tag{3}$$

where δ, ε and σ are dislocation density, microstrain and stacking fault respectively. Using the value of average crystallite size in Eq. (1), the value of dislocation density is found to be $1.11\times10^{-4}$ $nm^{-3}$. The dislocation density is large for fibrous particles and smaller for spherical shaped particles. Thus, the low value of dislocation density suggests spherical shape of $MoS_2$ nanoparticles. Dislocations distort a crystal lattice, causing stress and strain in the material. Thus, to estimate the structural characteristics of a material, it is essential to study these parameters. The value of microstrain in the sample is calculated by putting FWHM value of individual peaks in Eq. (2) and found to be $3.7\times10^{-4}$. The stacking default being a kind of planar defect also determines the properties of a material. Eq. (3). gives the value of stacking fault to be $7.4\times10^{-4}$.

There are some more methods which can be utilized to study crystallite size and strain including Williamson-Hall (W-H) (Fig. 2 (a)) and size strain plot (Fig. 2 (b)). The intercept of W-H plot gives the value of crystallite size to be 85.56 nm. The strain is given by the slope of W-H plot which is $1.198\times10^{-4}$. The slope and intercept of the size-strain plot also gives the value of crystallite size and strain respectively which are found to be 88.28 nm and $1.4\times10^{-6}$. The values of all the parameters obtained by different methods are summarized in Table 2.

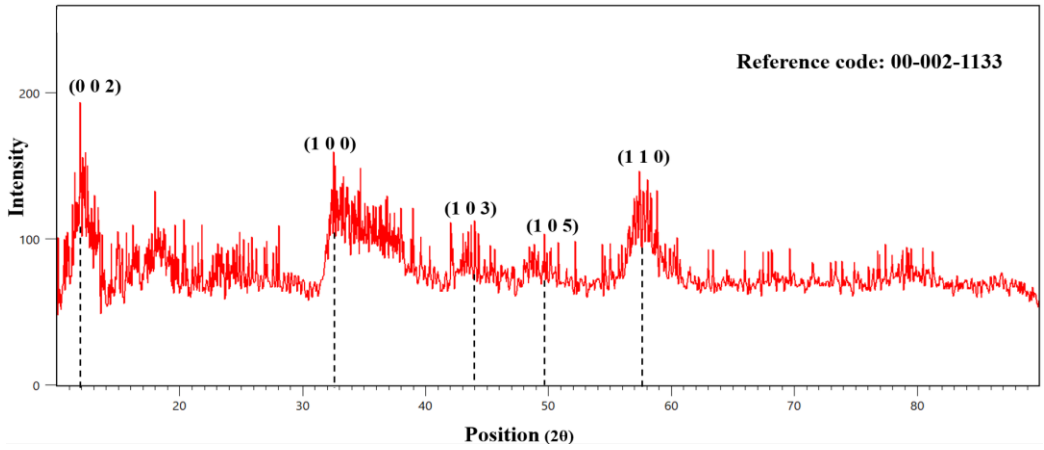


Fig. 1. XRD pattern of as-synthesized material

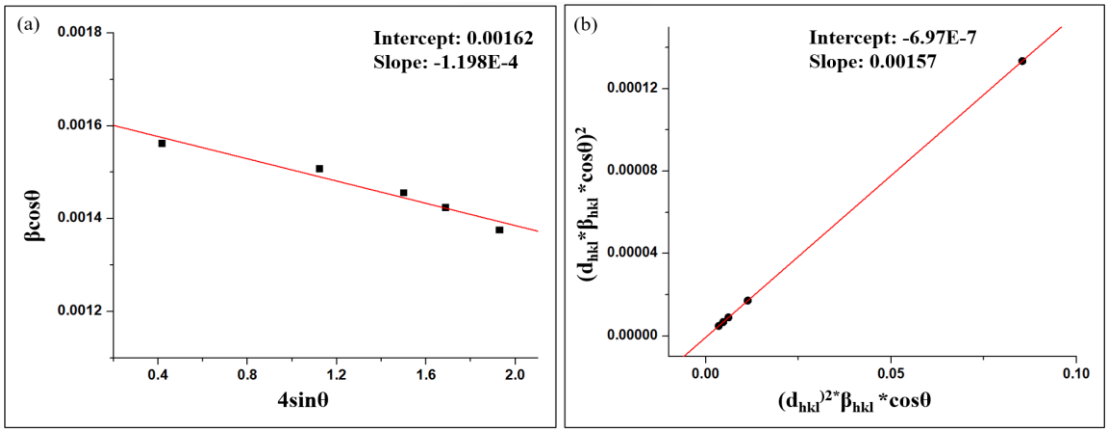


Fig. 2. (a) Williamson-Hall plot (b) size strain plot

Table 1. A comparison of calculated parameters of $MoS_2$ with standard values.

| | a (Å) | b (Å) | c (Å) | α (°) | β (°) | γ (°) |
|---|---|---|---|---|---|---|
| ICDD database value | 3.15 | 3.15 | 12.3 | 90 | 90 | 120 |
| Calculated value | 3.36 | 3.36 | 14.79 | 90 | 90 | 120 |

Table 2. The summary of calculated structural parameters of $MoS_2$.

| Parameters | Debye Scherrer equation | Williamson Hall plot | Size strain plot | Eq. 1, 2 or 3 |
|---|---|---|---|---|
| Crystallite size (nm) | 94.76 | 85.56 | 88.28 | - |
| Strain, € (×10$^{-4}$) | - | 1.198 | 0.014 | 3.7 |
| Dislocation density (nm$^{-3}$) (×10$^{-4}$) | - | - | - | 1.11 |
| Stacking fault (×10$^{-4}$) | - | - | - | 7.4 |

## 3.2. Optical studies

The optical studies of the as-synthesized material are studied using UV-vis spectrophotometer (Shimadzu 2600i UV-visible Spectrophotometer) which are the determining factors of a material's suitability for optoelectronic applications. Fig. 3 (a) shows the absorbance of as-synthesized $MoS_2$ in which the major absorption peaks are observed at 534, 543 and 562 nm. The absorbance data shows significant visible light absorption indicating its aptness for solar cell applications. The band gap of the material is found using Tauc plot (Fig. 3 (b)) taking the band gap to be direct. Extrapolating the linear part of the plot, the band gap is found to be 1.1 eV which is extremely close to the band gap of silicon. Thus, it propounds the usage of $MoS_2$ as a promising alternate of silicon in the solar cells.

*1) Refractive index*

It is another parameter determining the applicability of a material for solar cell applications. It can be estimated using the optical band gap acc to the following relation.

$$\frac{n^2-1}{n^2+2}=1-\sqrt{\frac{E_g}{20}} \tag{4}$$

Eq. (4) gives the value of refractive index as 3.28 which is comparable to the refractive index of silicon i.e., 3.88. Both values are near indicating the possible use of $MoS_2$ as an alternative of the conventional silicon.

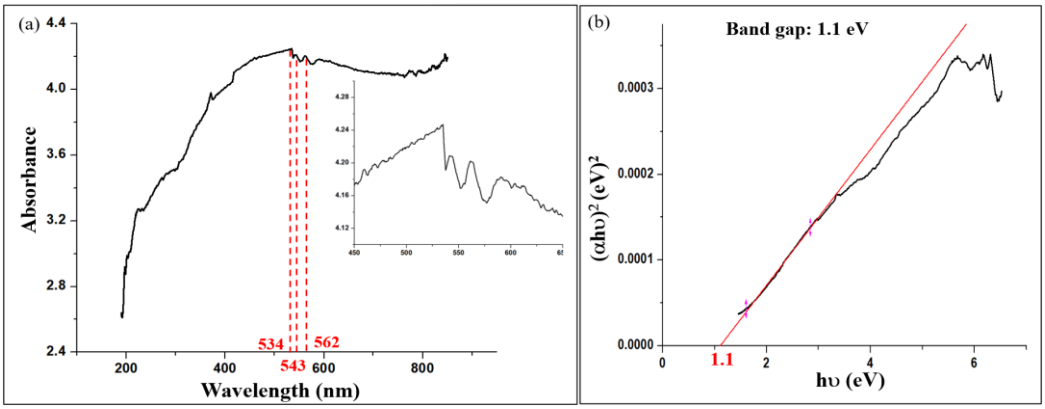


Fig. 3. (a) Absorbance of $MoS_2$ nanospheres (b) Tauc plot

## 3.3. Morphological analysis

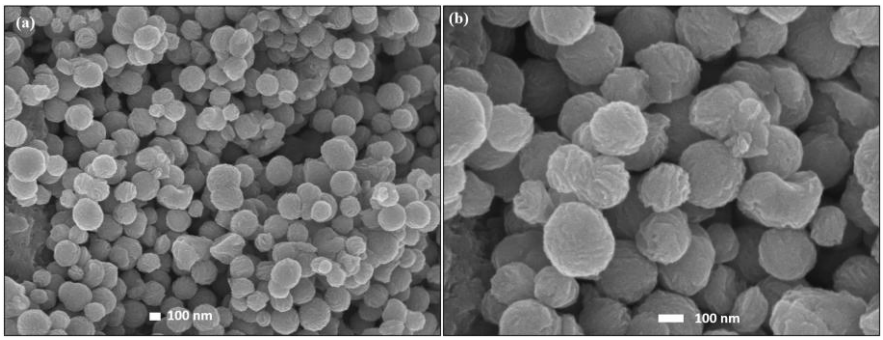


Fig. 4. (a, b) FESEM images of as-synthesized MoS2 nanospheres.

The surface morphology of the as-synthesized $MoS_2$ is investigated by using FESEM (JEOL, 20 kV). The SEM images (Fig. 4 (a, b)) show the formation of nanospheres on the surface of which layered structure of $MoS_2$ is visible. The surfactant added during synthesis has assembled the monolayers of $MoS_2$ giving it a spherical shape. The size of spheres varies from 100 to 250 nm which is larger than the crystallite size calculated by XRD analysis. It can be explained as a particle contains many crystallites in it making the particle size larger than the crystallite size. The composition of different elements is studied by EDX (Fig. 5 (b)) recorded along with for a selected area as depicted in Fig. 5(a). EDX pattern shows high intensity peaks of Mo and S confirming the presence of these elements in the sample.

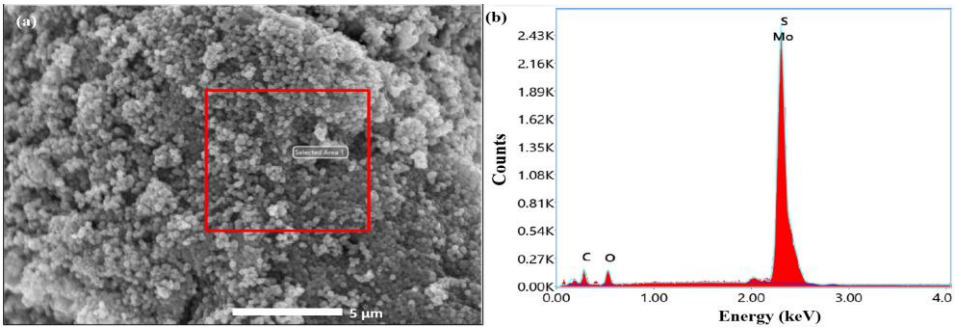


Fig. 5 . (a) FESEM image at large scale (b) corresponding EDX pattern of the selected area

### 3.4. Electrochemical study

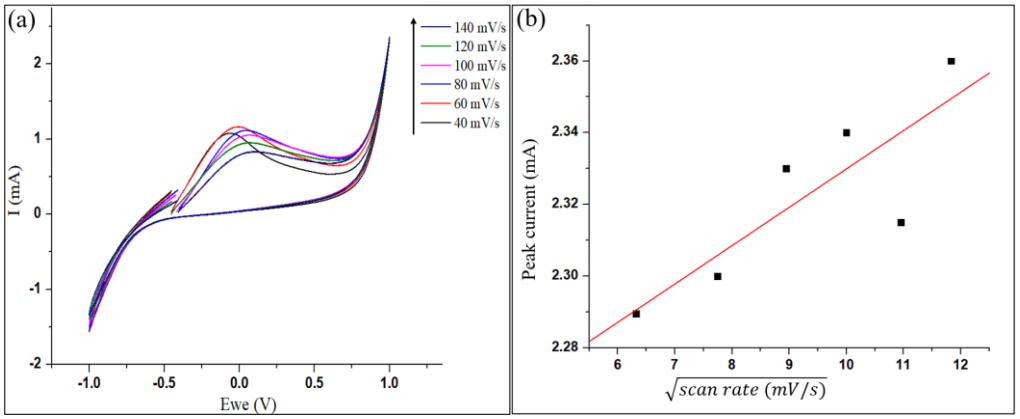


Fig. 6. (a) Cyclic voltammetry of $MoS_2$ nanospheres (b) Peak current variation with $\sqrt{scan\ rate}$

The electrochemical studies of the as-synthesized sample are performed to investigate the electrochemical behaviour of the material by studying the oxidation and reduction of the material. The change in current w.r.t the voltage is depicted by cyclic voltammetry analysis. The voltammogram is recorded at different scan rates ranging from 40 to 140 mV/s as shown in Fig. 6 (a). The peak current increases with the scan rate as stated by Rendles Sevick equation. The anodic peak current is 2.32 ± 0.04 mA and cathodic peak current is found to be 1.45±0.11 mA, the ratio of which is near to unity and thus indicating the electrochemical reversibility of the reaction.

The variation of peak current with square root of scan rate is studied in Fig. 6 (b), which shows the linear relationship between the two parameters. It shows the diffusion-controlled behavior of $MoS_2$ and confirms its usage for solar cell applications.

## 4. Conclusion

The microwave assisted hydrothermal route is successfully employed for the synthesis of $MoS_2$ nanospheres. XRD reveals the formation of hexagonal phase crystallites of size 90±5 nm. The optical studies

revealed the considerable absorbance in visible region along with the band gap of 1.1 eV and refractive index of 3.28 which are close to the values of silicon. The electrochemical analysis performed by cyclic voltammetry shows that the redox reaction taking place between electrodes is diffusion-controlled as there is linear relationship between peak current and $\sqrt{scan\ rate}$. The ratio of cathodic and anodic peak current sis near to unity, thus it also shows that the reaction is reversible. The degradation study of the film of $MoS_2$ nanospheres for 25 cycles at 60 mV/s shows that there is a little degradation over the time. Thus, the results indicate that the high efficiency solar cells can be fabricated using $MoS_2$ nanospheres.

## Conflict of Interest

The authors declare no conflict of interest.

## Author Contributions

Shreya Sharma conducted the research, analyzed the results and drafted the manuscript; Peeyush Phogat helped in the analysis and interpretation of the results. Sukhvir Singh reviewed the interpretation and the results. Sukhvir Singh and Prof. Ranjana Jha revised the manuscript critically. All authors had approved the final version.

## Acknowledgements

The authors are extremely grateful to the Vice-Chancellor, NSUT, Delhi, India for providing us the opportunity and resources to work in this encouraging environment where we can have substantial contribution to the research. One of the authors, Shreya would also like to acknowledge the financial support for research given by university as University Research Fellowship (URF).

## References

[1] Singh, E., Singh, P., Kim, K. S., Yeom, G. Y., and Nalwa, H. S. (Mar. 2019). Flexible Molybdenum Disulfide (MoS 2 ) Atomic Layers for Wearable Electronics and Optoelectronics. *ACS Appl Mater Interfaces*, *11(12)*, 11061–11105, doi: 10.1021/ACSAMI.8B19859/ASSET/IMAGES/MEDIUM/AM-2018-19859A_0028.GIF.

[2] Winer, W. O. (1967). Molybdenum disulfide as a lubricant: A review of the fundamental knowledge. *Wear*, *10(6)*, 422–452, doi: 10.1016/0043-1648(67)90187-1.

[3] Khatri, R. and Puri, N. K. (May 2020). Electrochemical study of hydrothermally synthesised reduced MoS2 layered nanosheets. *Vacuum*, 175, doi: 10.1016/J.VACUUM.2020.109250.

[4] Yadav, A., Shreya, and Puri, N. K. (2023). Preliminary observations of synthesized WS2 and various synthesis techniques for preparation of nanomaterials, 546–556, doi: 10.1007/978-981-16-9523-0_61.

[5] Benavente, E., Santa, Ana, M. A., Mendizábal, F., and González, G. (2002). Intercalation chemistry of molybdenum disulfide. *Coord Chem Rev*, *224(1–2)*, 87–109, doi: 10.1016/S0010-8545(01)00392-7.

[6] Sun, P., Zhang, W., Hu, X., Yuan, L., and Huang, Y. (Feb. 2014). Synthesis of hierarchical MoS2 and its electrochemical performance as an anode material for lithium-ion batteries. *J Mater Chem A Mater*, *2(10)*, 3498–3504, doi: 10.1039/C3TA13994H.

[7] Liu, Y., Zhong, Q., Chen, K., Zhou, J., Yang, X., and Chen, W. (Sept. 2017). Morphologies controllable synthesis of $MoS_2$ by hot-injection method: from quantum dots to nanosheets. *Journal of Materials Science: Materials in Electronics*, *28(18)*, 13633–13637,doi: 10.1007/S10854-017-7204-Z/FIGURES/3.

[8] Li, W. J., Shi, E. W., Ko, J. M., Chen, Z. Z., Ogino, H., and Fukuda, T. (Apr. 2003). Hydrothermal synthesis of MoS2 nanowires. *J Cryst Growth*, *250(3–4)*, 418–422, doi: 10.1016/S0022-0248(02)02412-0.

[9] Shreya, Yadav, A., Khatri, R., Jain, N., Bhandari, A., and Puri, N. K. (2023). Double zone thermal CVD and plasma enhanced CVD systems for deposition of films/coatings with eminent conformal coverage.

*Advances in Manufacturing Technology and Management, 273–283*, doi: 10.1007/978-981-16-9523-0_31.